Journal of Autoimmunity 140 (2023) 103097

Contents lists available at ScienceDirect

Journal of Autoimmunity

journal homepage: www.elsevier.com/locate/jautimm

Non-classical circulating monocytes expressing high levels of *microsomal prostaglandin E2 synthase-1* tag an aberrant IFN-response in systemic sclerosis

Gonzalo Villanueva-Martin [a], Marialbert Acosta-Herrera [a,b], Elio G. Carmona [a,b], Martin Kerick [a], Norberto Ortego-Centeno [b,c], Jose Luis Callejas-Rubio [b], Norbert Mages [d], Sven Klages [d], Stefan Börno [d], Bernd Timmermann [d], Lara Bossini-Castillo [e,f,1,*], Javier Martin [a,1,**]

[a] Department of Cell Biology and Immunology, Institute of Parasitology and Biomedicine López-Neyra, CSIC, Granada, Spain
[b] Systemic Autoimmune Disease Unit, Hospital Clínico San Cecilio, Instituto de Investigación Biosanitaria Ibs. GRANADA, Granada, Spain
[c] Department of Medicine, University of Granada, Instituto de Investigación Biosanitaria Ibs. GRANADA, Granada, Spain
[d] Sequencing Core Facility, Max Planck Institute for Molecular Genetics, 14195, Berlin, Germany
[e] Department of Genetics and Biotechnology Institute, Biomedical Research Centre (CIBM), University of Granada, 18100, Granada, Spain
[f] Advanced Therapies and Biomedical Technologies (TEC-14), Biosanitary Research Institute Ibs. GRANADA, 18016, Granada, Spain

ARTICLE INFO

Handling Editor: M.E. Gershwin

Keywords:
Systemic sclerosis
Single-cell transcriptome
scRNA-seq
Monocyte
CD14

ABSTRACT

Systemic sclerosis (SSc) is a complex disease that affects the connective tissue, causing fibrosis. SSc patients show altered immune cell composition and activation in the peripheral blood (PB). PB monocytes (Mos) are recruited into tissues where they differentiate into macrophages, which are directly involved in fibrosis. To understand the role of $CD14^+$ PB Mos in SSc, a single-cell transcriptome analysis (scRNA-seq) was conducted on 8 SSc patients and 8 controls. Using unsupervised clustering methods, $CD14^+$ cells were assigned to 11 clusters, which added granularity to the known monocyte subsets: classical (cMos), intermediate (iMos) and non-classical Mos (ncMos) or type 2 dendritic cells. NcMos were significantly overrepresented in SSc patients and showed an active IFN-signature and increased expression levels of *PTGES*, in addition to monocyte motility and adhesion markers. We identified a SSc-related cluster of *IRF7*+ *STAT1*+ iMos with an aberrant IFN-response. Finally, a depletion of M2 polarised cMos in SSc was observed. Our results highlighted the potential of PB Mos as biomarkers for SSc and provided new possibilities for putative drug targets for modulating the innate immune response in SSc.

1. Introduction

Systemic sclerosis (SSc) is a chronic life-threatening immune-mediated disease (IMD), which is characterised by an imbalanced immune response, endothelial damage and progressive fibrosis of the skin and internal organs [1]. Clinical manifestations among patients are highly heterogeneous, involving different extents of fibrosis, the appearance of autoantibodies against different nuclear structures and the onset of clinical complications or comorbidities [1]. SSc patients are classified into two major clinical subtypes: limited cutaneous SSc (lcSSc), if fibrosis is restricted to specific areas of the body (i.e. face and limbs), and diffuse cutaneous SSc (dcSSc), if fibrosis is generalised and affects mostly the torso and the proximal regions of the limbs [1]. From a geneticist point of view, SSc is classified as a complex disorder, as it is triggered by unknown environmental factors in genetically predisposed individuals [2]. Large genetic studies have contributed to establish 27 *loci* as firm genetic players in SSc susceptibility [3].

Both the adaptive and innate responses are chronically active and aberrant in SSc patients [4]. In this regard, innate myeloid cells that act as antigen presenting cells (APCs) [5] have been shown to be involved in pathological tissue scarring and fibrosis in SSc patients [6]. Moreover, alterations of the macrophage compartment have been suggested as essential drivers of connective tissue fibrosis in SSc [7]. Notably, in the early stages of SSc skin fibrosis, macrophages show a proinflammatory

* Corresponding author. Department of Genetics and Biotechnology Institute, Biomedical Research Centre (CIBM), University of Granada, 18100, Granada, Spain.
** Corresponding author. Department of Cell Biology and Immunology, Institute of Parasitology and Biomedicine López-Neyra, CSIC, 18016, Granada, Spain.
E-mail addresses: lbossinicastillo@ugr.es (L. Bossini-Castillo), javiermartin@ipb.csic.es (J. Martin).
[1] These authors contributed equally.

https://doi.org/10.1016/j.jaut.2023.103097
Received 18 May 2023; Received in revised form 10 August 2023; Accepted 16 August 2023
Available online 24 August 2023

M1 and/or M2 concomitant profile that might progress towards a M1/M2 disequilibrium in later stages [8]. Furthermore, a new set of CXCL4-induced macrophages, which might be linked with profibrotic skills, has been identified in SSc patients. However, their exact role in the disease is yet to be defined [9].

Recently, the study of the molecular mechanisms leading to anomalous macrophage behaviour in SSc-affected tissues has reached an unprecedented level of detail thanks to the improvements of single cell transcriptome (scRNA-seq) technologies [6,10], which focused on the tissue-resident fibroblast, lymphocyte and macrophage populations [6,11,12]. Regarding macrophages, pioneer studies have identified a highly proliferative SSc-specific M2 macrophage subpopulation in the lungs distinguished by the expression of osteopontin (*SPP1*) [10], which induces profibrotic characteristics in the fibroblasts [13]. In the case of skin macrophages, scRNA-seq experiments of dcSSc skin have singled out a macrophage subpopulation characterised by the expression of high levels of Fcγ receptor IIIA (*FCGR3A*, also known as CD16) [6].

Interestingly, myeloid populations are not only a tissue-resident lineage, but also circulate in the peripheral blood (PB) as monocytes (Mos) [4]. Due to the systemic nature of the disease, the monocyte compartment of SSc patients has abnormal biophysical properties and increased proportions of circulating inflammatory non-classical Mos (ncMo) [14–17]. Moreover, SSc Mos have been reported to increase their adhesion by reducing the expression of *CD52* [18] and upregulating *CCR3* [19] as a response to type I IFN. Moreover, circulating myeloid cells in the blood of SSc patients, especially those with a severe disease, have a gene expression profile that combines M1 and M2 surface markers [20–22].

Nevertheless, scRNA-seq technologies have not been applied to comprehensively characterise circulating $CD14^+$ Mos in the blood of SSc patients. Therefore, we will investigate the composition and the cell subtype-specific expression profiles of the monocyte compartment in SSc at the highest resolution by analysing the single cell transcriptomes of more than 94,000 $CD14^+$ PB cells from 8 patients affected with SSc and 8 controls.

2. Methods

2.1. Patient description

The study cohort consisted of 16 women. All individuals were of self-reported European ancestry and of similar age (average age SSc = 60; average age controls = 59), 8 of them were diagnosed with SSc and the remaining 8 were unaffected. Patients fulfilled the diagnostic criteria for the disease proposed by ACR [23] and were classified into limited cutaneous or diffuse cutaneous SSc according to the criteria proposed by LeRoy [24,25]. Clinical information of the patients, as well as their serological profile and drug treatment are shown in Supplementary Table 1. All participants were selected from the *Hospital Universitario San Cecilio* (Granada, Spain) by qualified staff and they signed a written consent before being enrolled in the study. All samples were irreversibly anonymised.

2.2. Cell suspension protocol

Thirty millilitres of PB of each participant were collected in EDTA tubes (Greiner #4550356) and processed for cryopreservation within 1 h of extraction. $CD14^+$ cells were isolated at the Instituto de Parasitología y Biomedicina López-Neyra (Granada, Spain). Next, plasma was separated from peripheral blood mononuclear cells (PBMCs) using Ficoll® Paque Plus (Merk #GE 17-1440-02) density gradients in Leucosep centrifuge tubes (Greiner #227290). Positive selection of $CD14^+$ cells was performed using a magnetic bead kit (Stem Cell Easy Step, ref #17858) by following the protocol established by the manufacturer. The $CD14^+$ cells accounted for more than 86.5% of the cells in the samples as confirmed by flow-cytometry analyses and high *CD14* mRNA expression was later confirmed at the single cell level (Supplementary Fig. 1). Then, $CD14^+$ cell suspensions were cryopreserved in 10% DMSO (Merk D2438) and 90% foetal bovine serum (FBS, Gibco #10082-147) medium and frozen in a −80 °C ultrafreezer at a controlled rate for at least 24 h using a CoolCell container (Corning # 432000). Samples were kept in liquid nitrogen for long term storage.

2.3. Single cell RNA-sequencing library generation

To perform single cell whole transcriptome sequencing (scRNA-seq), we used the Next GEM technology by 10× Genomics. Samples were assayed following the manufacturer's instructions for the following kits: Chromium Next GEM Chip G Single Cell Kit (10xGenomics, PN-1000127) and Chromium Next GEM Single Cell 5′ Library and Gel Bead Kit v1.1 (10xGenomics, PN-1000165_a). Subsequently, the generated cDNA libraries were sequenced using the NovaSeq 6000 platform (Illumina) with S2 and SP chemistry v1.5. The previously described settings allowed us to obtain an average of 85.85% of reads in cells, with an average of 31,847 reads per cell. The sequencing reads were aligned to the GRCh38 genome build and unique molecular identifiers (UMI) were processed by the 10× Cell Ranger Single Cell Software Suite (v3.0.0) using default parameters, with an average of 1658 genes identified per cell.

2.4. Single cell RNA-sequencing data analysis

Cell Ranger results were imported into Scanpy (v1.8.2) [26] in Python (v3.8.1). All individuals passed the established quality filters. Any cell with less than 500 genes, more than 10% of reads mapping in mitochondrial genes or more than 30% of reads mapping in ribosomal genes was removed. In addition, to avoid doublets, any cell with more than 3000 detected genes was discarded. The *MTRNR2L8* gene was found to be aberrantly expressed in only one individual and was, therefore, excluded from the analysis. Altogether 94,525 $CD14^+$ cells, and 22,637 genes passed the filters.

Normalisation by library size and logarithmic transformation was applied to the resulting UMIs for each cell that passed QC, using the scanpy tools and their default settings. Next, the scanpy cell cycle analysis tool was used, using a list of publicly available cell cycle-related genes [27], assigning to each cell a cell cycle phase. We used 5000 highly variable genes (HVG) in our downstream analyses, which were selected at this point. To ensure that the results were not biassed by biological variation, the following parameters were regressed out using the scanpy regress_out function: number of UMIs per cell, proportion of reads in mitochondrial and ribosomal genes and cell cycle (S phase and G2M phase). Finally, the resulting data were scaled to unit variance and values exceeding standard deviation 10 were clipped.

Scaled data were then used to perform principal component analysis (PCA), and we used the first 20 PCs to perform a Batch Balanced k-Nearest Neighbour (BBkNN) integration graph, using the individuals as a correction key. This BBkNN graph was later used for embedding and visualisation with the Uniform Manifold Approximation and Projection (UMAP) algorithm [28], as well as for unsupervised clustering with the Leiden algorithm [29]. All the samples were properly integrated and similar clustering results were obtained using alternative algorithms (Supplementary Figs. 2 and 3). The CellTypist package (v1.2.0) [30] was used to identify non-monocytic cells, mainly lymphoid cells, which were removed from the data. Additionally, apoptotic cells were identified on the basis of a panel of apoptosis markers and discarded from further analysis. Finally, 94,525 cells remained in the dataset, on which the analyses described above were repeated.

Finally, the 11 clusters defined by the unsupervised Leiden clustering algorithm were assigned to known $CD14^+$ cell subsets based on genetic markers from the literature (Supplementary Fig. 4). However, each cluster was analysed individually to prevent interpretation bias based on previous immunological cell subset definitions.

2.4.1. Differential gene expression

In order to identify genes that can be used as cluster-specific marker genes and to analyse differential gene expression (DE) between cells in the same cluster but originated from different conditions, we applied the rank_genes_groups function implemented in scanpy. Scanpy then calculated differential expression for each gene and ranked them based on their Z-score and the underlying p-value. A Wilcoxon statistical test was applied for DE calculation and the Benjamini-Hochberg FDR (FDR <0.1) strategy was applied as a correction method. Log2 fold changes were also calculated per group as implemented in the previously mentioned function.

2.4.2. Pathway enrichment analysis

The top 10% cluster marker genes and DE genes were considered for pathway enrichment analysis. The enrichment analysis was performed using the Gene Ontology (GO), Kyoto Encyclopedia of Genes and Genomes (KEGG) and Reactome databases using R package EnrichR (v3.1.0). A p-value <0.05 after FDR correction was established as a statistical significance threshold.

2.4.3. Trajectory analysis

To explore potential cell trajectories, we relied on the methods implemented in Monocle3 (v3.0) [31]. For this purpose, the object was first converted to a Seurat (v4.3.0) [32] object, using the SeuratData (v0.2.2) and SeuratDisk (v0.0.09020) packages. The sample was then downsampled to 9,000 cells, and then converted to a cell data set object with the Seurat function as.cell_data_set. The effect sizes of the raw counts were then estimated and the cluster_cell function was applied to perform the clustering and partitioning of the data in order to calculate the cell trajectories. Finally, the pseudotime branches were inferred with the learn_graph function. Based on the expression of genes related to the transdifferentiation of Mos to macrophages (*FCGR3A*, *CSF1R* and *RHOC*), cluster 0 was chosen as the pseudotime root (this cluster corresponded to cluster 1 according to the monocle3 clustering).

We used the graph_test and find_gene_modules functions implemented in Monocle3 to identify modules of genes that changed with the pseudotime. We applied a multiple testing correction [33] on the results and, if a gene had a q value ≤ 0.05 and a Moran's I (a measure of the degree of correlation) greater than 0.05, it was considered to be significantly associated with the pseudotime trajectory[34].

To perform the diffusion mapping, an unsupervised dimensionality reduction analysis package Destiny (v3.12.0) [35] was used. Previously, the SingleCellExperiment package (v1.20.0) [36] was needed to adapt the Seurat object exported from Scanpy.

3. Results

3.1. Peripheral blood CD14$^+$ monocytes show a IFN signature in SSc

In order to comprehensively characterise the pathological alterations of the transcriptome at the single cell level in PB Mos of SSc patients, we analysed the transcriptome of 94,525 CD14$^+$ cells. As shown in Supplementary Table 1, our study cohort was composed of 8 women affected by SSc (6 with lcSSc and 2 with dcSSc) and 8 non-affected women. Patients had several years of disease duration and all of them presented Raynaud's phenomenon and similar drug treatment. The majority of the recruited patients had gastrointestinal complications, but only some of them showed pulmonary involvement. The patients and controls were matched by ethnicity and age.

CD14$^+$ Mos represent a ~10% of the leukocytes in PB [37] and the number of isolated CD14$^+$ cells per sample was consistent between the controls and the SSc patients, but also between patients with lcSSc and patients with dcSSc (Supplementary Table 2). We detected not only CD14^{high} but also CD14^{low}CD16^{high} cells, which corresponded to the non-classical monocyte population [38]. Therefore, the analysed cells showed a modest to high *CD14* expression (Supplementary Fig. 1), and an average of 1,658 genes per cell were detected.

After QC, we generated an integrated data set combining the SSc and control CD14$^+$ monocyte transcriptomes. We observed that all samples were evenly distributed (Supplementary Fig. 2), but each condition showed a distinct density pattern with qualitative differences between SSc and controls, as well as between lcSSc and dcSSc (Fig. 1A). Moreover, the comparison of the average gene expression between controls and SSc, lcSSc or dcSSc identified the overexpression in cases of 2,665, 2,640 and 1,057 genes, respectively (Fig. 1B; Supplementary Figs. 5A and 5B; Supplementary Tables 3–5).

The top DE genes (DEG) in SSc compared with controls included interferon response genes, such as *IFITM3*, *IRF1*, *IFITM2* and *IFI6*. Nevertheless, we also observed monocyte migration markers, for example *LGALS2*, and *TMSB10*. Additionally, antigen presentation molecules were remarkably DE, i.e. *HLA-A* and *HLA-DRB5* (Fig. 1B; Supplementary Table 3). Furthermore, relevant SSc-associated transcription factors, as *STAT1* and *KLF6,* showed a significantly increased expression in patients with SSc (Fig. 1B; Supplementary Table 3). In fact, pathway enrichment analysis highlighted that these SSc upregulated genes were enriched in several proinflammatory mechanisms such as: response to type I and type II IFN, Toll-like receptor signalling and Class I MHC-mediated antigen processing and presentation (Supplementary Table 6). It should also be noted that overexpressed genes in SSc included several key players of the innate immune response, the interferon-induced guanylate binding protein (GBP) family: *GBP1, GBP2, GBP3, GBP4* and *GBP5* (Supplementary Table 3) [39].

The comparison between lcSSc patients and controls revealed that the general biological pathways enriched with DE genes were very similar to the observed trends for SSc (Supplementary Table 4). However, we detected subtype specific overexpression of genes encoding proteins of the complement cascade (such as, *CFD*) in lcSSc (Supplementary Table 4). On the contrary, patients with dcSSc showed increased levels of the monocyte activation related genes, such as *LYZ, CSF3R* (Supplementary Table 5).

Additionally, when lcSSc and dcSSc were compared, we identified 1,156 genes upregulated in lcSSc and 636 genes upregulated in dcSSc (Supplementary Table 7). Compared with dcSSc, the lcSSc subtype showed an overexpression of some interferon response genes (*i.e. S100A4*, *IFNGR2*), subtype-specific increased levels of negative regulators of dendritic cell differentiation (*TMEM176A* and *TMEM176B*) [40], and an enhanced antigen presentation profile with several HLA genes amongst the most DEG (Fig. 1C; Supplementary Table 7). On the other hand, the top dcSSc upregulated genes compared to lcSSc were involved in monocyte migration (*SELL* [41], *CD52* [42], *VCAN* [43]) and in monocyte differentiation, *CLEC12A* [44] (Fig. 1B and C, Supplementary Table 7). These DEGs were also enriched in interferon-related pathways and, additionally in intercellular communication, for example: immunoregulatory interactions between a lymphoid and a non-lymphoid cell (Supplementary Table 8). In addition, RUNX3-mediated immune response and migration were in the top enriched pathways (Supplementary Table 8).

3.2. Interferon activated non-classical CD16$^+$ RHOC + monocytes express high levels of microsomal prostaglandin E2 synthase-1 in SSc

Eleven cell clusters were defined on the basis of transcriptional similarity by implementing the community detection Leiden algorithm in an UMAP (Fig. 2A). All the individuals contributed to all clusters (Fig. 2B) and there was no cluster restricted to SSc or the SSc subtypes (Supplementary Fig. 2). Notably, the implementation of the Louvain algorithm on a t -distributed stochastic neighbour embedding (t-SNE) visualisation resulted in similar clusters (Supplementary Fig. 3).

Panels of known membrane surface markers allowed us to manually annotate clusters into the three major monocyte subsets: cMo (*CD14*$^+$/*SELL*, 5 clusters), iMo (*HLA-DRA/CD74*$^+$, 4 clusters) and ncMo (*FCGR3A*$^+$/*C1QA*$^+$, 1 cluster) (Fig. 2C; Supplementary Fig. 4). We also

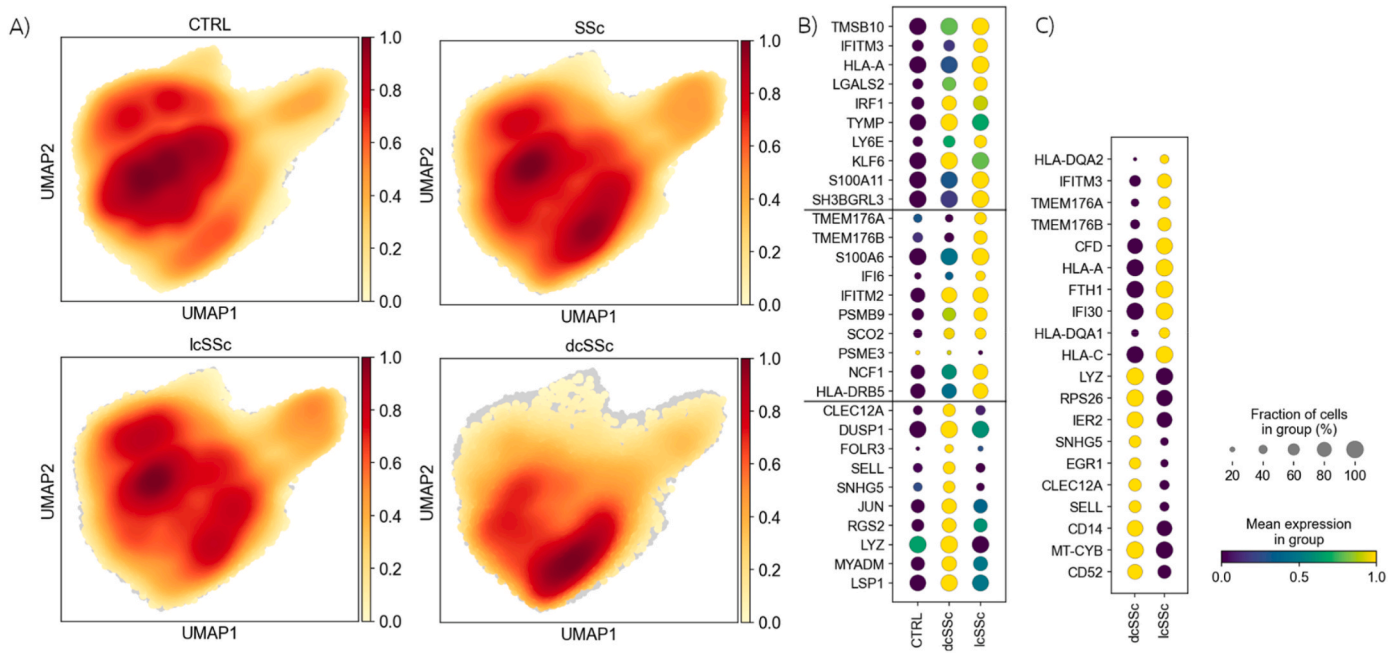

Fig. 1. Cellular density and differential gene expression in SSc subtypes and controls. A) UMAP plots showing cellular density of CTRL, lcSSc, and dcSSc. Colour gradient indicates increasing density. B) Top 10 differentially expressed genes in SSc vs. CTRL, lcSSc vs. CTRL, and dcSSc vs. CTRL. C) Top 10 differentially expressed genes between lcSSc and dcSSc, and vice versa. Point size represents the fraction of cells per group expressing each gene, and colour represents the expression level of each gene in each group. SSc: Systemic Sclerosis; lcSSc: limited cutaneous SSc; dcSSc: diffuse cutaneous SSc; CTRL: controls.

detected a DC2 population (*CD1C*$^+$ *FCER1A*$^+$/*CLEC10A*$^+$, 1 cluster).

We observed that the ncMo compartment (cluster 7) was significantly overrepresented in SSc patients, and especially in lcSSc cases (Fig. 2D; Supplementary Fig. 6). NcMo are CD16$^+$ cells, which was consistent with cluster 7 showing the highest expression of the CD16 encoding gene, i.e. *FCGR3A* (Fig. 2D, Supplementary Fig. 4). This ncMo cluster was characterised by high expression of *LST1*, which was also overexpressed in the SSc cells of this cluster (Fig. 2D, Supplementary Table 9). *LST1* encodes a *trans*-membrane and soluble protein induced by immune response against bacteria and associated with the inhibition of lymphocyte proliferation [45]. Moreover, cell motility-related genes, such as *COTL1* [46] and *RHOC* [47], were also clear markers for this subset of Mos (Fig. 2D, Supplementary Table 9). It should be noted that *RHOC* was differentially expressed between SSc and controls, as well as being overexpressed in lcSSc cases compared with dcSSc patients. Although *RHOC* was a cluster marker (logFold change = 4.3) for ncMos (cluster 7), it was differentially expressed between SSc and controls in ncMo but also in the nearby subsets of antigen-presenting iMos (clusters 2 and 3) (Fig. 3A; Supplementary Tables 3, 7, 9 and 10).

The interferon signature in ncMo was clear with several interferon induced genes, such as *IFITM3* and *IFITM2* in the top gene markers and differentially overexpressed in SSc patients (Supplementary Tables 9 and 10). The DEGs with the largest log fold changes (logFold change >1.5) included very promising *loci* related to SSc-associated fibrosis. For example, *PTGES*, which encodes an inducible microsomal enzyme that acts downstream from cyclooxygenase-2 and catalyses the prostaglandin 2 (PGE2) synthesis [48] or *CEACAM3*, a cellular adhesion molecule [49], were exclusively DE in this cluster of ncMo (Fig. 3A; Supplementary Table 10). Finally, several complement system genes, such as *C1QA*, *C1QB*, *C1QC* and *CSF1R*, showed the greatest fold change increases in the ncMo cluster compared with the rest of the CD14$^+$ cells (Fig. 3A; Supplementary Table 10).

3.3. Migration of M2 polarised monocytes is altered in SSc

We observed that cluster 9 was underrepresented in individuals affected by SSc, which was especially visible in lcSSc patients (Fig. 2D). Cluster 9, a cMo subset, was characterised by a high expression of genes related to cell adhesion and migration, such as *VCAN*, *CD36*, *VIM* and *ITGB2* (Supplementary Table 9). Moreover, pathway enrichment analysis of the marker genes showed that the most relevant pathways also included cell surface interactions at vascular wall and several pathways related to extracellular matrix composition, (such as chondroitin sulfate/dermatan sulfate metabolism, diseases associated with glycosaminoglycan metabolism, etc.) and fibrosis (interleukin-4 and interleukin-13 signalling) [50] (Supplementary Table 11).

Remarkably, this cluster showed markers of monocyte activation (*AHNAK* [51], *DDX5* [52,53], and *CD44* [54]). Especially, we identified several markers of polarisation towards a M2 profibrotic phenotype [55], i.e. *AHR* [51], *TGFB1* and *CD163* [56] (Fig. 3B and Supplementary Fig. 7). Additionally, we observed some M1 markers among the cluster 9 markers (Supplementary Fig. 7), such as *NLRP3* and *IL1B* (Supplementary Table 9) [57]. However, *NLRP3* had a higher expression in controls than in SSc (logFold change = −0,23) and *IL1B* was not differentially expressed (Supplementary Table 9). Finally, the SSc cMos in this cluster showed a high overexpression of the S100A gene family (*S100A8*, *S100A6*, *S100A10*, *S100A9*) and other interferon-response genes (*IRF1*, *IFITM3*, *IFITM2*) (Fig. 3B; Supplementary Table 10).

Then, we analysed the composition and characteristics of an iMo IFN signature-related cluster: cluster 8. SSc patients contributed more to this iMo cluster, which was marked by very high expression of genes related to IFN induction, such as *ISG15*, *MX1*, *MX2* and *IFI6* (Figs. 2D and 3C). It should be noted that two master regulators of IFN-mediated immune activation, which have been previously involved in SSc pathogenesis and appeared DE in our comparison between all cells from SSc patients versus the control cells, *IRF7* and *STAT1*, marked exclusively this cluster (Supplementary Tables 4, 9 and 10). As expected by the cluster marker genes, DE analysis showed that the highest over-expression corresponded to MHC-I (*HLA-A*) and MHC-II (*HLA-DRB5*) genes and members of the S100A family (*S100A8/S100A9*, *S100A6* and *S100A11*), all markers of monocyte activation and inflammation (Fig. 3C).

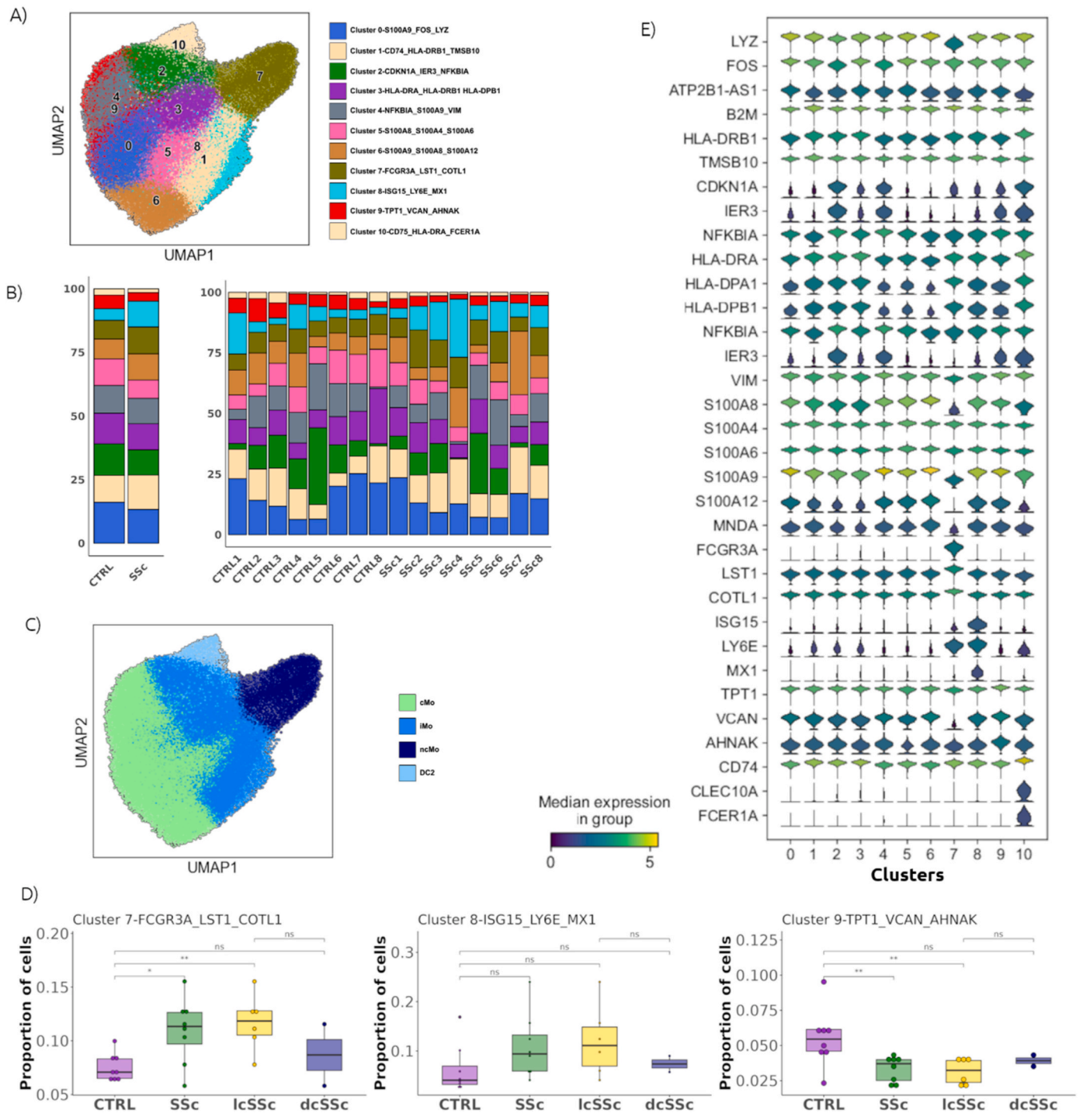

Fig. 2. A) UMAP of the 11 CD14$^+$ cell clusters from SSc and control samples, obtained using Leiden clustering and labelled from 0 to 10. B) Proportion of cells in each cluster by condition (CTRL or SSc) and by individual. Each cluster is represented by the same colour as in panel A. C) UMAP with the clusters classified and coloured according to the assigned cell type based on their expression of different marker genes. Clusters 0, 5, 4, 6, and 9 were classified as cMo; clusters 1, 2, 3, and 8 as iMo; cluster 7 as ncMo; and cluster 10 as DC2. D) Boxplots representing the cell proportions for CTRL, SSc, lcSSc, and dcSSc (from left to right) in clusters 7, 8, and 9. E) Violin plots of the top 3 DE genes of each cluster vs the rest, with colours representing the expression level in each group. cMo: classical monocytes; iMo: intermediate monocytes; ncMo: non-classical monocytes; DC2: dendritic cells type 2; DE: differential expression.

3.4. The expression of SSc genetic risk loci is altered in SSc CD14$^+$ monocytes

Considering our success in establishing *IRF7* and *STAT1*, known SSc genetic risk factors, as cluster specific markers, we checked the expression of other known SSc risk *loci* [3].

We observed that *CSK*, *RAB2A*, *TSPAN32*, *GRB2*, *IL12RB1*, *IRF8*, *DDX6*, and *TNIP1* were DE in the comparison between all the SSc cells and all the control cells (Supplementary Table 3). All of them were upregulated in SSc, but only *CSK*, a kinase of the Src family that interacts with the immune-related *PTPN22 locus*, was significantly upregulated in lcSSc versus dcSSc (Supplementary Table 7). Remarkably, for some of these *loci* we were able to characterise cluster specific DEs.

We observed that the expression of *CSK* was increased in patient

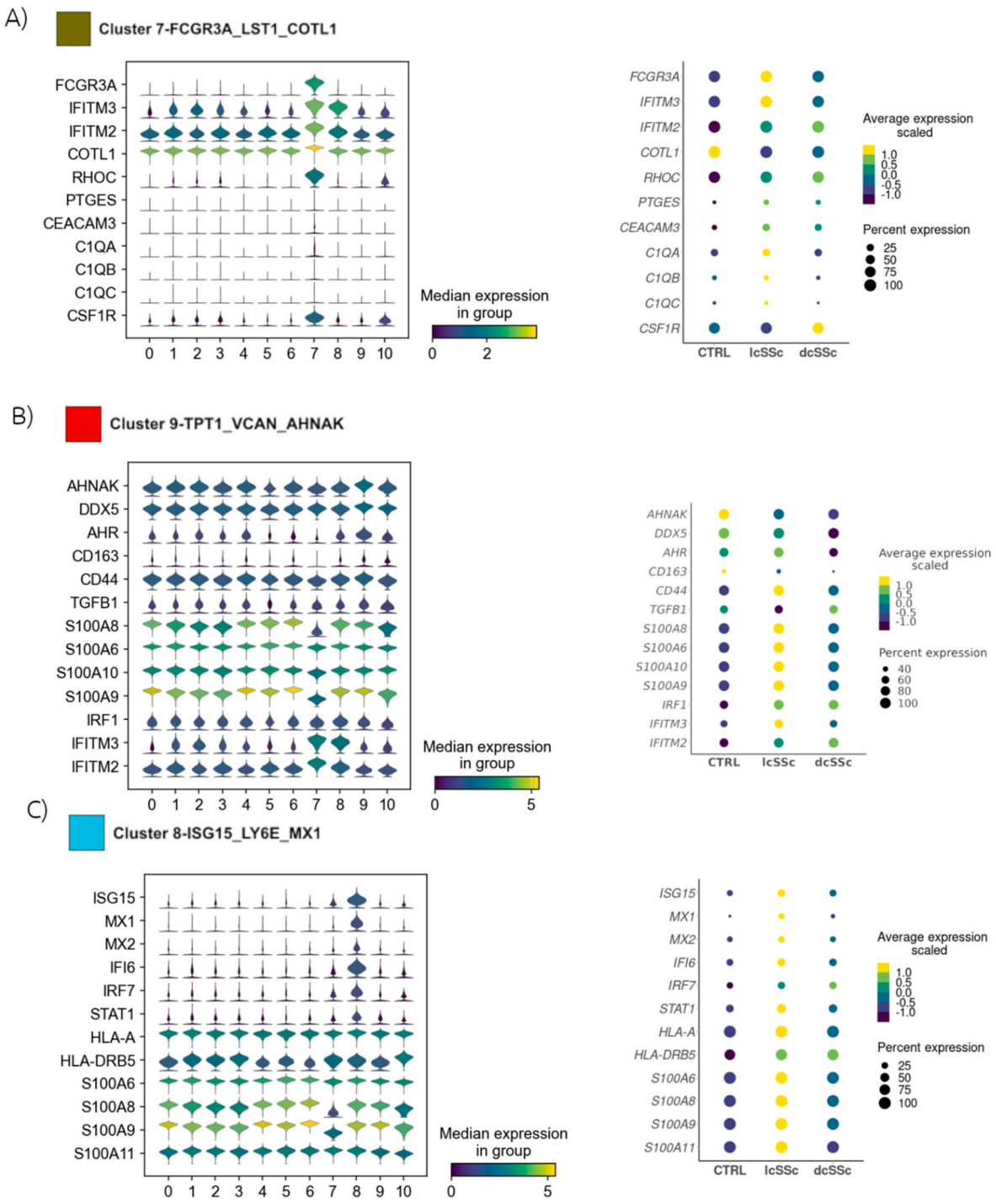

Fig. 3. Violin plots and dotplots of gene expression in A) cluster 7, B) cluster 9 and C) cluster 8. The height of each violin indicates the cell proportion of each cluster and colours indicate expression levels and DE between controls and lcSSc and dcSSc is depicted in the dotpots.

cMos (clusters 0, 4 and 5) and iMos (clusters 1, 2, 3 and 8), but not ncMos or DC2 (Supplementary Table 10). On the contrary, *RAB2A locus*, which encodes a Rab GTPase involved in intracellular vesicle trafficking, showed DE scattered in several monocyte clusters identified as either cMos (clusters 0 and 5), iMos (cluster 2) or ncMos (cluster 7).

As opposed to *IRF7*, which was a marker gene for clusters 7 and 8 but showed a generalised DE in several monocyte clusters, *IRF8* (also involved in transcriptional regulation via IFN) was a common marker for several clusters and it was upregulated in SSc in two cMo clusters (clusters 0 and 3) (Supplementary Tables 9 and 10). It should be noted that recent reports have identified a $CD14^+$ cell-exclusive 3D chromatin interaction between a SSc-associated SNP, which was located in the vicinity of *IRF8* (rs11117420), and the promoter of this *locus* using Hi-C study in $CD14^+$ Mos obtained from SSc patient blood [58].

The *GRB2 locus* was exclusively overexpressed in the SSc cells that belonged to cluster 0, and *ARHGAP31* and *TSPAN32* were significantly upregulated in SSc only in cluster 3 (Supplementary Table 10).

Notably, *IL12RB1*, which had been previously identified as a genetic risk *locus* for SSc [3,59], was highly expressed in the inflammatory SSc ncMos (Supplementary Table 9).

Finally, we observed that only one gene, *ANXA6*, located near the *TNIP1* SSc genetic susceptibility locus [60], showed a decreased

expression in SSc patients compared to controls in all the defined clusters (logFold change ranging 0.17-0.69) (*Supplementary Tables 3–5*). Additionally, *ANXA6* was a cluster marker for all the cMo clusters, except for cluster 5 (*Supplementary Table 9*). Interestingly, a decreased expression of *ANXA6* and a physical interaction between the *ANXA6* promoter and a nearby enhancer located in a *TNIP1* intron have been previously described in SSc CD4$^+$ lymphocytes [61]. Moreover, the alleles of rs3792783, a SSc-associated SNP located in *TNIP1* [60], correlated both with the methylation status of the enhancer and with *ANXA6* expression [61]. Therefore, our findings support further investigation of the relevance of an altered expression of this locus in the context of CD14$^+$ and especially in cMos in SSc patients.

3.5. *IRF7+ STAT1+ intermediate monocytes show a distinctive IFN-response in SSc*

Then, we explored the relationship between the different monocyte clusters and studied the existence of specific gene modules or cellular states that correlated with SSc. Consequently, we carried out a pseudotime analysis.

We observed that the monocyte clusters seemed to gradually differentiate from cMos towards either ncMos or DC2s with iMos acting as a crossroads (Fig. 4A). The trajectory root was located in cMo clusters, such as CD14+, *SELL*+, and *CD36*$^+$ (Supplementary Fig. 4). However, the progression towards the endpoints relied on the expression of genes such as *FCGR3A* (CD16) and *FCER1A*, both markers of ncMos and DC2s, respectively (Fig. 4B).

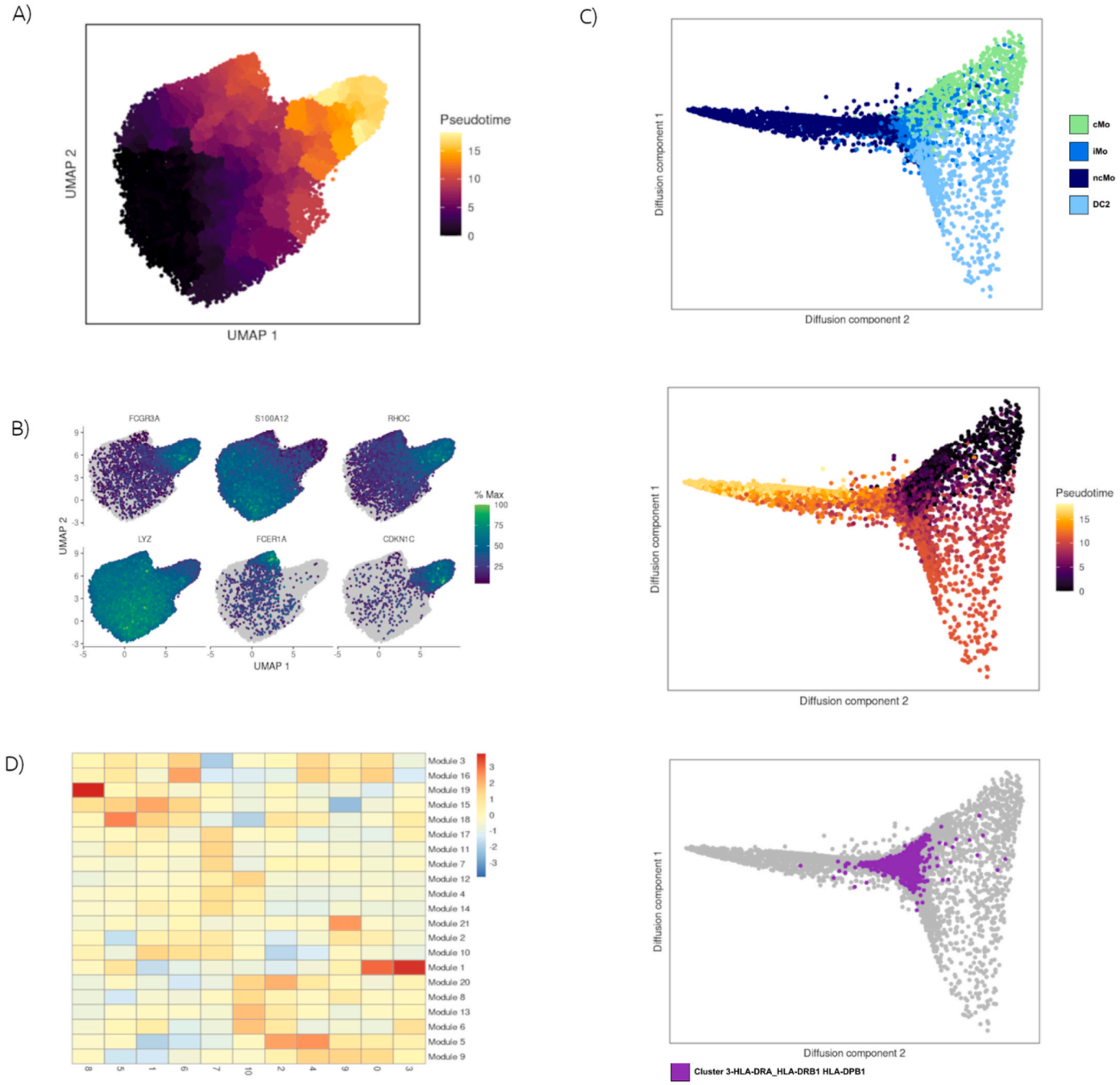

Fig. 4. A) UMAP showing CD14$^+$ cells from SSc and CTRLs coloured by pseudotime. B) Expression of the top 6 genes in the CD14$^+$ pseudotime C) Diffusion maps coloured by cell type, pseudotime, and cluster 3 (from top to bottom). D) Heatmap of gene module expression per cluster. Numbers indicate clusters.

Moreover, the cMo clusters located at the start of the trajectory were clearly characterised by markers of an IFN-mediated response, i.e. *S100A12* (Fig. 4B), that have already been addressed as SSc biomarkers above. Nevertheless, the trajectory ended in the ncMo cluster and it was driven by the expression of two SSc-related markers: *RHOC* and *CDKN1C* (Supplementary Tables 3, 9 and 10). Both genes further suggested an overreactivity of ncMos in SSc, since the protein encoded by *RHOC* is key in the regulation of cell motility and *CDKN1C*, also known as *P57*, acts as a cyclin-dependent tumour suppressor.

Then, we took into account that the estimated pseudotime seemed to have at least two different endpoints (Fig. 4A) and decided to calculate a diffusion map to identify the branching points and connections between the different cell clusters. The diffusion map confirmed that ncMos and DC2s were established as two clearly different branches and, although the different iMos clusters were located between the cMos, and the ncMos or the DCs, cluster 3 appeared as an intersection between cMos and their polarisation to ncMos or DC2s (Fig. 4B and C; Supplementary Fig. 8). Although the transit from cMos to DC2s seemed gradual, the polarisation from cMos to ncMos looked linear with cluster 3 as a bottleneck (Fig. 4C). Cluster 3 was characterised by a very high expression of HLA class II genes, which were also upregulated by the SSc cells in this cluster (Supplementary Tables 9 and 10).

Finally, we identified modules of co-expressed genes in the trajectory and we focused on those that showed a cluster specific pattern (Fig. 4D). Module 1 was characteristic of the previously mentioned crossroads iMos cluster, cluster 3 (Fig. 4D). This gene module was shaped by a variety of genes such as *MTHFR* (coding gene for the methylenetetrahydrofolate reductase enzyme) and *CELA2A* (which encodes a chymotrypsin like elastase) (Supplementary Table 12). But pathway enrichment suggested that this module might be correlated with signalling via IL1R (including *loci* such as *JUN, TGFB2, IL1RN*) and might be involved in the altered proportions of monocyte subsets in SSc.

On the contrary, module 19 was integrated by *ISG15* together with several proteins of the GBP family (*GBP1, GBP2, GBP3*) and IFN-induced genes (*IFI6, IFI44, IFI44L*) that were previously described as DEG in SSc (Supplementary Tables 3 and 12). *ISG15* was a specific marker gene for cluster 8 (*IRF7*+ *STAT1*+ iMos), which was overrepresented in SSc and showed the highest expression of module 19 (Figs. 2D, 3C and 4D), which allowed us to restrict this particular IFN-response to a specific subset of SSc iMos.

4. Discussion

In specific pathogenic conditions, as in the SSc fibrotic tissue, macrophages are essential for the activation of profibrotic myofibroblasts [4,5]. However, still in PB circulation, SSc Mos show altered composition and expression profiles [16,62]. As opposed to affected tissue, blood is abundant and easily accessible, and it is often an appropriate biomarker for disease monitoring. Interestingly, single cell transcriptome analysis of PB immune cells and Mos has been fruitful to identify unique cell populations and disease activity-related profiles in IMDs [63,64]. Despite their central role in SSc pathogenesis, the circulating Mo compartment transcriptome had never been characterised at the single cell level before.

This study analysed the largest number of the circulating $CD14^+$ cells (over 90,000 cells) in SSc patients compared to healthy controls. We prioritised identifying rare cell clusters and comprehensively characterising the differences between clusters over addressing interindividual variability. The reported findings provided valuable insights into $CD14^+$ cellular heterogeneity and dynamics, and to identify disease markers in SSc. Nevertheless, the main limitation of the study is the number of studied individuals (8 SSc patients and 8 CTRLs) and further replication in larger independent cohorts are needed to validate the subtype-specific findings. Therefore, we consider that the comparisons comprising disease subtypes should be treated with caution, especially in the case of dcSSc.

Reassuringly, we observed an overrepresentation of inflammatory ncMos (cluster 7) (Fig. 2D) as previously described [15,17]. Recently, Carvalheiro et al. described an increased frequency of CXCL10-producing ncMo in SSc and an elevated frequency of CXCL8-producing ncMos upon stimulation [65]. We observed that the ncMos in Cluster 7 exhibited a very high *CXCL10* expression (logFold change = 1.3) compared to other clusters (Supplementary Table 9) and that *CXCL8* expression was increased in SSc ncMos and iMo clusters as well (Supplementary Table 10).

Additionally, the identified ncMo cluster in our dataset showed a very high expression of known IFN-induced markers produced by myeloid cells in SSc fibrotic skin, such as *S1008A/S100A9*, which stimulate keratinocyte secretion of CXCL2 and CXCL3, as well as IL-6 (a known SSc hallmark) [66]. Consistent with a IFN-mediated effect in ncMos, SSc patient treatment with anifrolumab (a human monoclonal antibody against the interferon-α/β receptor subunit 1) in clinical trials correlated with a decreased TGF-β fibrosis and reduced expression levels of some of the ncMo markers observed in our study, such as *TGB1*, *CXCL10* and *B2M* [67] (Supplementary Tables 9–10). Therefore, the main role of the IFN-mediated ncMo activation might be to influence the cytokine profile of ncMos.

We also hypothesise that IFN might affect ncMo migration. Of particular significance is the upregulation of ncMo tissue migration markers, i.e. *CX3CR1* and *CEACAM3* [49,68] (Supplementary Tables 9–10). *CEACAM3* and several members of its family had been previously associated with SSc as well as correlated with interstitial lung disease, but these previous reports related *CEACAM3* to cMos [66]. Contrarily, our data showed that *CEACAM3* was an exclusive marker for ncMos, while *CEACAM4* was a marker for cMos and iMos clusters (Fig. 3B, Supplementary Tables 9 and 10). The transcriptomic signature for increased motility that we describe would match a recent study that investigated the biophysical properties of ncMos in SSc patients [16]. Matei et al. found that the ncMo of patients were pathologically more activated and exhibited biophysical characteristics that rendered them more prone to vascular migration and tissue infiltration [16]. While a mechanistic explanation for the IFN signal in SSc ncMos was out of the scope of our study, our findings are consistent with an imbalanced cytokine production and migration of ncMos in this disorder.

Additionally, we discovered that the SSc inflammatory ncMos show increased expression of prostaglandin E synthase, which is also known as mPGES-1 (microsomal Prostaglandin E Synthase-1) and encoded by *PTGES*, in a cluster-specific fashion (Supplementary Table 9). Although the cytosolic prostaglandin E synthase gene (*PTGES3*) was a cluster marker for ncMos, only *PTGES* was overexpressed in SSc ncMos compared to control ncMos (Supplementary Table 10). Prostaglandin-2 injections are used as an effective treatment for Raynaud's phenomenon in SSc patients due to its effect as a vasodilator [69], but PGE2 has a dual effect in inflammation. Depending on its association with different G-protein coupled PGE2 receptor subtypes, PGE2 shows an anti--inflammatory and pro-resolving activity or it mediates proinflammatory non-resolving immune activation [70]. Remarkably, mPGES-1 is an inducible microsomal enzyme that has been associated with pathological overproduction of PGE2 [71]. We would like to highlight that fibroblast from *PTGES* null mice were resistant to the bleomycin skin fibrosis SSc model, and that *PTGES* has been involved in monocyte/macrophage activation via PPARG (a known SSc genetic risk factor [72]), after stimulation with IL-17 [73,74]. Therefore, considering the recent advances in PTGES-specific inhibition, targeting this molecule specifically in SSc inflammatory ncMos might provide new drug targets for this disease.

Notably, a scRNA-seq analysis of SLE PBMCs reported that the Mo compartment showed the highest interferon-stimulated gene expression increase [75], concordantly with the large IFN-signature gene expression profile observed in our study. Interestingly, a SLE-specific cluster that was integrated by Mos expressing high levels of IFN-induced genes had similar cluster marker genes than a SSc-related cluster, the ISG15 +

LY6E + iMo cluster (cluster 8) (Fig. 2D, Supplementary Table 9). Moreover, this cluster showed relevant resemblance to a $C1q^{hi}$ monocyte cluster that was recently identified in a scRNA-seq study in PBMCs of patients with Behçet's disease (BD) [76]. Although we did not find a $C1q^{hi}$ cluster in SSc, the $C1q^{hi}$ Mos in BD showed hybrid characteristics between the inflammatory SSc ncMos, which showed the largest expression of complement genes, and SSc-related iMos (cluster 8) (Supplementary Table 9). In BD, the STAT1-mediated response to IFNɣ was correlated with *IRF1* [77] in this cluster. Notably, *IRF1* was one of the most DEG in all the SSc monocyte clusters, especially in dcSSc patients, and a marker for cluster 8 (Supplementary 3–5, 10 and 9). In addition to *IRF1*, SSc iMos in cluster 8 showed an *IRF7* signal. Of note, genetic variants in the *IRF7* locus were associated with SSc [78] and the *STAT1/IRF7* axis has also been implicated in fibroblast differentiation into myofibroblasts in SSc skin [11]. Therefore, we consider that our findings support that inflammatory ncMos and IFN-activated iMos in SSc have an aberrant response to IFN that might predispose them to a biassed macrophage polarisation.

As mentioned above, we observed several IFN-induced genes, such as several S100A family members or IFITM proteins, significantly DE in both clinical subtypes of SSc patients (Supplementary Tables 3–5). There is increasing evidence that suggests that high levels of these molecules might be associated with a deregulated monocyte proliferation and migration [66,79,80]. Considering that IFITM proteins, especially *IFITM3*, have been shown to be negatively regulated by mTOR inhibitors [81], our findings might support the emerging role of mTOR inhibition as a promising drug target for SSc [82] and particularly for lcSSc patients, who showed the highest *IFITM3* mRNA levels (Supplementary Table 8).

High levels of galectin-1 and galectin-3 (encoded by *LGALS1* and *LGALS3*, respectively) were previously reported in the sera of SSc patients [83], but for the first time, we found overexpression of *LGALS2* in SSc (Supplementary Tables 3–5 and 10). Remarkably, gal-2 is predominantly expressed in the gastrointestinal tract and it can bind to the surface of different immune lineages [84], including Mos and macrophages [85]. Nevertheless, unlike other galectins, gal-2 is expressed in immune cells only by the myeloid lineage [86]. Furthermore, gal-2 acts through a CD14/toll-like receptor (TLR)-4 pathway (a well-established SSc-related deregulated pathway in fibrotic skin and lung [87]) by altering Mo polarisation towards a proinflammatory phenotype [88]. Considering that a gal-2 antibody treatment has shown promising capacities of altering the polarisation of macrophages in a murine atherosclerosis model [89], these findings might also open new windows for treatment in SSc.

M2 macrophages are known to be increased in SSc skin [90] and to produce high levels of TGF-β. TGF-β is a key profibrotic factor [91], which is known to activate Mos more intensely in SSc than in healthy controls [92] and to polarise macrophages towards a profibrotic M2 phenotype [93]. Interestingly, we observed a cMo cluster (cluster 9) that showed markers of M2 polarisation, such as *CD163* and *TGFB1*, and which was depleted in patients with SSc (Fig. 2D and Supplementary Fig. 7). Furthermore, we observed that the top cluster 9 markers included *AHR* and *CD36* (Supplementary Fig. 7, Supplementary Table 9), which might be informative of the role of these Mos in the tissue. AHR has a key role in M1/M2 polarisation and is known to promote M2 polarisation and suppress M1 development [94]. CD36 is a relevant apoptotic cell receptor and phagocytosis promoter that has been linked with an M2 phenotype and increased fibrosis [95]. Additionally, *IL1B*, a M1 marker that was also present in this cluster (Supplementary Table 9), has been shown to also mediate the activation of M2 macrophages in highly fibrotic skin tissue [96].

All the described findings connect cluster 9 with M2 polarised Mos being actively recruited to affected connective tissue and are consistent with an altered M1/M2 balance in SSc blood with lower M1 polarisation levels in SSc. The underrepresentation of a highly activated cluster in an IMD might seem counterintuitive, but we hypothesise that it would be due to an increased migration of M2-polarised Mos to SSc-affected tissue in patients. Remarkably, increased levels of monocyte migration markers, such as *VCAN* and *ITGB2*, were observed in this cluster (Fig. 3B and Supplementary Table 9). *VCAN* (also known as versican) expression have been related with increased circulating Mo migration in SSc [97]. Besides, *ITGB2* has been identified as a SSc-associate monocyte gene and found to be upregulated in SSc skin macrophages [38].

Finally, SSc bleomycin mouse models showed that the modulation of M2 cytokine production by *PDE4* inhibition decreased skin fibrosis [98], and we observed high levels of expression of *PDE4* in cluster 9 and other cMos clusters (Supplementary Table 9). Therefore, we propose that specifically blocking the extravasation of the novel TPT1+ VCAN + AHNAK + cMo cluster into challenged tissue might benefit SSc patients.

5. Conclusions

In conclusion, we performed the most detailed characterisation of the $CD14^+$ Mo compartment in SSc to date. We confirmed an overrepresentation of $CD16^+$ ncMos at single cell level. Inflammatory SSc ncMos showed a high IFN-response signature and the upregulation of PGE_2 synthesis, monocyte adhesion markers and complement genes. We also identified an aberrant IFN-response in *IRF7*+ *STAT1*+ SSc iMos and, finally, we observed a depletion of M2 polarised cMos in SSc. These results reinforced the role of PB Mos as SSc biomarkers and provided new windows for clinical monitoring and drug targeting.

Funding

This work was supported by the grant P18-RT-4442 funded by *Consejería de Transformación Económica, Industria, Conocimiento y Universidades, Junta de Andalucía*. "Red de Investigación Cooperativa Orientada a Resultados en Salud'' (RICOR, RD21/0002/003). 115565. LBC was supported by the Spanish Ministry of Science and Innovation through the *Juan de la Cierva Incorporación*' program (Grant ref. IJC2018-038026-I, funded by MCIN/AEI/10.13039/501,100,011,033), which includes FEDER funds. MAH is a recipient of a Miguel Servet fellowship (CP21/00132) from the *Instituto de Salud Carlos III* (Spanish Ministry of Science and Innovation). GV-M was funded by the Grant PRE2019-087586 funded by MCIN/AEI/10.13039/501,100,011,033 and by "ESF Investing in your future".

Contributors

GVM: data analysis, data interpretation, manuscript drafting, revision and approval; MAH: data interpretation, manuscript revision and approval; EGC: data analysis, manuscript revision and approval; MK: data interpretation, manuscript revision and approval; NOC: data acquisition, manuscript revision and approval; JLCR: data acquisition, manuscript revision and approval; NM: experiments and manuscript revision and approval; SK: data analysis; SB: data analysis, manuscript revision and approval; BT: manuscript revision and approval; LBC: study design, data analysis, manuscript drafting, revision and approval; JM: study design, data interpretation, manuscript drafting, revision and approval.

Ethical approval

An ethical protocol was prepared with consensus across all partners and was approved by the local ethical committee of the clinical recruitment centre. The study adhered to the standards set by the International Conference on Harmonization and Good Clinical Practice (ICH-GCP), and to the ethical principles that have their origin in the Declaration of Helsinki (2013). The protection of the confidentiality of records that could identify the included subjects is ensured as defined by the EU Directive 2001/20/EC and the applicable national and international requirements relating to data protection in each participating

country. This study was approved by the Ethical Committee "CEIM/CEI Provincial de Granada", and the CSIC Ethical Committee.

Code availability

All the codes used for processing and analyzing the data in this study were compiled into a single publicly available GitHub repository [https://github.com/gonv/scRNA-seq_SSc_CD14_nb].

Data availability

Data will be made available on request.

Acknowledgements

This research is part of the doctoral degree awarded to GV-M, within the Biomedicine program from the University of Granada entitled "Deciphering the genetic basis of systemic sclerosis". We would like to thank Sofia Vargas and Gemma Robledo for their excellent technical assistance and Gonzalo Borrego-Yaniz for his collaboration in the illustration of the cells for the figures. We also appreciate the controls and the affected individuals who generously provided the samples for these studies. Funding for open access charge: Universidad de Granada/CBUA.

Appendix A. Supplementary data

Supplementary data to this article can be found online at https://doi.org/10.1016/j.jaut.2023.103097.

References

[1] E.R. Volkmann, K. Andréasson, V. Smith, Systemic sclerosis, Lancet 401 (2023) 304–318.
[2] L. Bossini-Castillo, E. López-Isac, M.D. Mayes, J. Martín, Genetics of systemic sclerosis, Semin. Immunopathol. 37 (2015) 443–451.
[3] E. López-Isac, M. Acosta-Herrera, M. Kerick, S. Assassi, A.T. Satpathy, J. Granja, M. R. Mumbach, L. Beretta, C.P. Simeón, P. Carreira, N. Ortego-Centeno, I. Castellvi, L. Bossini-Castillo, F.D. Carmona, G. Orozco, N. Hunzelmann, J.H.W. Distler, A. Franke, C. Lunardi, G. Moroncini, A. Gabrielli, J. de Vries-Bouwstra, C. Wijmenga, B.P.C. Koeleman, A. Nordin, L. Padyukov, A.M. Hoffmann-Vold, B. Lie, R. Ríos, J.L. Callejas, J.A. Vargas-Hitos, R. García-Portales, M.T. Camps, A. Fernández-Nebro, M.F. González-Escribano, F.J. García-Hernández, M. J. Castillo, M.A. Aguirre, I. Gómez-Gracia, B. Fernández-Gutiérrez, L. Rodríguez-Rodríguez, P. García de la Peña, E. Vicente, J.L. Andreu, M. Fernández de Castro, F. J. López-Longo, L. Martínez, Fonollosa, A. Guillén, G. Espinosa, C. Tolosa, A. Pros, M. Rodríguez-Carballeira, F.J. Narváez, M. Rubio-Rivas, Ortiz-Santamaría, A. B. Madroñero, M.A. González-Gay, B. Díaz, L. Trapiella, A. Sousa, M.V. Egurbide, P. Fanlo-Mateo, L. Sáez-Comet, F. Díaz, E. Beltrán Hernández, J.A. Román-Ivorra, E. Grau, J.J. Alegre-Sancho, M. Freire, F.J. Blanco-García, N. Oreiro, T. Witte, A. Kreuter, G. Riemekasten, P. Airó, C. Magro, A.E. Voskuyl, M.C. Vonk, R. Hesselstrand, S. Proudman, W. Stevens, M. Nikpour, J. Zochling, J. Sahhar, J. Roddy, P. Nash, K. Tymms, M. Rischmueller, S. Lester, T. Vyse, A.L. Herrick, J. Worthington, C.P. Denton, Y. Allanore, M.A. Brown, T.R.D.J. Radstake, C. Fonseca, H.Y. Chang, M.D. Mayes, J. Martin, GWAS for systemic sclerosis identifies multiple risk loci and highlights fibrotic and vasculopathy pathways, Nat. Commun. 10 (2019) 1–14.
[4] A. Lescoat, V. Lecureur, J. Varga, Contribution of monocytes and macrophages to the pathogenesis of systemic sclerosis: recent insights and therapeutic implications, Curr. Opin. Rheumatol. 33 (2021) 463–470.
[5] G. Kania, M. Rudnik, O. Distler, Involvement of the myeloid cell compartment in fibrogenesis and systemic sclerosis, Nat. Rev. Rheumatol. 15 (2019) 288–302.
[6] D. Xue, T. Tabib, C. Morse, Y. Yang, R.T. Domsic, D. Khanna, R. Lafyatis, Expansion of Fcγ receptor IIIa-positive macrophages, ficolin 1-positive monocyte-derived dendritic cells, and plasmacytoid dendritic cells associated with severe skin disease in systemic sclerosis, Arthritis Rheumatol. 74 (2022) 329–341.
[7] R. Bhandari, M.S. Ball, V. Martyanov, D. Popovich, E. Schaafsma, S. Han, M. ElTanbouly, N.M. Orzechowski, M. Carns, E. Arroyo, K. Aren, M. Hinchcliff, M. L. Whitfield, P.A. Pioli, Profibrotic activation of human macrophages in systemic sclerosis, Arthritis Rheumatol. 72 (2020) 1160–1169.
[8] B. Skaug, D. Khanna, W.R. Swindell, M.E. Hinchcliff, T.M. Frech, V.D. Steen, F. N. Hant, J.K. Gordon, A.A. Shah, L. Zhu, W. Jim Zheng, J.L. Browning, A.M. S. Barron, M. Wu, S. Visvanathan, P. Baum, J.M. Franks, M.L. Whitfield, V. K. Shanmugam, R.T. Domsic, F.V. Castelino, E.J. Bernstein, N. Wareing, M. A. Lyons, J. Ying, J. Charles, M.D. Mayes, S. Assassi, Global skin gene expression analysis of early diffuse cutaneous systemic sclerosis shows a prominent innate and adaptive inflammatory profile, Ann. Rheum. Dis. 79 (2020) 379–386.
[9] M. van der Kroef, T. Carvalheiro, M. Rossato, F. de Wit, M. Cossu, E. Chouri, C.G. K. Wichers, C.P.J. Bekker, L. Beretta, N. Vazirpanah, E. Trombetta, T.R.D. J. Radstake, C. Angiolilli, CXCL4 triggers monocytes and macrophages to produce PDGF-BB, culminating in fibroblast activation: implications for systemic sclerosis, J. Autoimmun. 111 (2020), 102444.
[10] A. Papazoglou, M. Huang, M. Bulik, A. Lafyatis, T. Tabib, C. Morse, J. Sembrat, M. Rojas, E. Valenzi, R. Lafyatis, Epigenetic regulation of profibrotic macrophages in systemic sclerosis-associated interstitial lung disease, Arthritis Rheumatol. 74 (2022) 2003–2014.
[11] T. Tabib, M. Huang, N. Morse, A. Papazoglou, R. Behera, M. Jia, M. Bulik, D. E. Monier, P.V. Benos, W. Chen, R. Domsic, R. Lafyatis, Myofibroblast transcriptome indicates SFRP2hi fibroblast progenitors in systemic sclerosis skin, Nat. Commun. 12 (2019) 4384.
[12] A.M.Gaydosik, T.Tabib, R.Domsic, D.Khanna, R.Lafyatis, P.Fuschiotti, Single-cell transcriptome analysis identifies skin-specific T-cell responses in systemic sclerosis, Ann. Rheum. Dis. 80 (2021) 1453–1460.
[13] X. Gao, G. Jia, A. Guttman, D.J. DePianto, K.B. Morshead, K.-H. Sun, N. Ramamoorthi, J.A. Vander Heiden, Z. Modrusan, P.J. Wolters, A. Jahreis, J. R. Arron, D. Khanna, T.R. Ramalingam, Osteopontin links myeloid activation and disease progression in systemic sclerosis, Cell Rep Med 1 (2020), 100140.
[14] L. Schneider, N.A. Marcondes, V. Hax, I.F. da Silva Moreira, C.Y. Ueda, R. R. Piovesan, R. Xavier, R. Chakr, Flow cytometry evaluation of CD14/CD16 monocyte subpopulations in systemic sclerosis patients: a cross sectional controlled study, Adv Rheumatol 61 (2021) 27.
[15] A. Lescoat, V. Lecureur, M. Roussel, B.L. Sunnaram, A. Ballerie, G. Coiffier, S. Jouneau, O. Fardel, T. Fest, P. Jégo, CD16-positive circulating monocytes and fibrotic manifestations of systemic sclerosis, Clin. Rheumatol. 36 (2017) 1649–1654.
[16] A.-E. Matei, M. Kubánková, L. Xu, A.-H. Györfi, E. Boxberger, D. Soteriou, M. Papava, J. Prater, X. Hong, C. Bergmann, M. Kräter, G. Schett, J. Guck, J.H. W. Distler, Biophysical phenotyping of circulating immune cells identifies a distinct monocyte-driven signature in systemic sclerosis, Arthritis Rheumatol 75 (2023) 768–781.
[17] C. Gur, S.-Y. Wang, F. Sheban, M. Zada, B. Li, F. Kharouf, H. Peleg, S. Aamar, A. Yalin, D. Kirschenbaum, Y. Braun-Moscovici, D.A. Jaitin, T. Meir-Salame, E. Hagai, B.K. Kragesteen, B. Avni, S. Grisariu, C. Bornstein, S. Shlomi-Loubaton, E. David, R. Shreberk-Hassidim, V. Molho-Pessach, D. Amar, T. Tzur, R. Kuint, M. Gross, O. Barboy, A. Moshe, L. Fellus-Alyagor, D. Hirsch, Y. Addadi, S. Erenfeld, M. Biton, T. Tzemach, A. Elazary, Y. Naparstek, R. Tzemach, A. Weiner, A. Giladi, A. Balbir-Gurman, I. Amit, LGR5 expressing skin fibroblasts define a major cellular hub perturbed in scleroderma, Cell 185 (2022) 1373–1388.e20.
[18] M. Rudnik, F. Rolski, S. Jordan, T. Mertelj, M. Stellato, O. Distler, P. Blyszczuk, G. Kania, Regulation of monocyte adhesion and type I interferon signaling by CD52 in patients with systemic sclerosis, Arthritis Rheumatol. 73 (2021) 1720–1730.
[19] R. Lee, C. Reese, B. Perry, J. Heywood, M. Bonner, M. Zemskova, R.M. Silver, S. Hoffman, E. Tourkina, Enhanced chemokine-receptor expression, function, and signaling in healthy African American and scleroderma-patient monocytes are regulated by caveolin-1, Fibrogenesis Tissue Repair 8 (2015) 11.
[20] S. Soldano, A.C. Trombetta, P. Contini, V. Tomatis, B. Ruaro, R. Brizzolara, P. Montagna, A. Sulli, S. Paolino, C. Pizzorni, V. Smith, M. Cutolo, Increase in circulating cells coexpressing M1 and M2 macrophage surface markers in patients with systemic sclerosis, Ann. Rheum. Dis. 77 (2018) 1842–1845.
[21] A. Lescoat, A. Ballerie, S. Jouneau, O. Fardel, L. Vernhet, P. Jego, V. Lecureur, M1/M2 polarisation state of M-CSF blood-derived macrophages in systemic sclerosis, Ann. Rheum. Dis. 78 (2019) e127.
[22] A.C. Trombetta, S. Soldano, P. Contini, V. Tomatis, B. Ruaro, S. Paolino, R. Brizzolara, P. Montagna, A. Sulli, C. Pizzorni, V. Smith, M. Cutolo, A circulating cell population showing both M1 and M2 monocyte/macrophage surface markers characterizes systemic sclerosis patients with lung involvement, Respir. Res. 19 (2018) 186.
[23] Preliminary criteria for the classification of systemic sclerosis (scleroderma). Subcommittee for scleroderma criteria of the American Rheumatism Association Diagnostic and Therapeutic Criteria Committee, Arthritis Rheum. 23 (1980) 581–590.
[24] E.C. LeRoy, T.A. Medsger Jr., Criteria for the classification of early systemic sclerosis, J. Rheumatol. 28 (2001) 1573–1576.
[25] E.C. LeRoy, C. Black, R. Fleischmajer, S. Jablonska, T. Krieg, T.A. Medsger Jr., N. Rowell, F. Wollheim, Scleroderma (systemic sclerosis): classification, subsets and pathogenesis, J. Rheumatol. 15 (1988) 202–205.
[26] F.A. Wolf, P. Angerer, F.J. Theis, SCANPY: large-scale single-cell gene expression data analysis, Genome Biol. 19 (2018) 15.
[27] E.Z. Macosko, A. Basu, R. Satija, J. Nemesh, K. Shekhar, M. Goldman, I. Tirosh, A. R. Bialas, N. Kamitaki, E.M. Martersteck, J.J. Trombetta, D.A. Weitz, J.R. Sanes, A. K. Shalek, A. Regev, S.A. McCarroll, Highly parallel genome-wide expression profiling of individual cells using nanoliter droplets, Cell 161 (2015) 1202–1214.
[28] L. McInnes, J. Healy, J. Melville, UMAP: Uniform Manifold Approximation and Projection for Dimension Reduction, Arxiv(2018).
[29] V.A. Traag, L. Waltman, N.J. van Eck, From Louvain to Leiden: guaranteeing well-connected communities, Sci. Rep. 9 (2019) 5233.
[30] C. Domínguez Conde, C. Xu, L.B. Jarvis, D.B. Rainbow, S.B. Wells, T. Gomes, S. K. Howlett, O. Suchanek, K. Polanski, H.W. King, L. Mamanova, N. Huang, P. A. Szabo, L. Richardson, L. Bolt, E.S. Fasouli, K.T. Mahbubani, M. Prete, L. Tuck, N. Richoz, Z.K. Tuong, L. Campos, H.S. Mousa, E.J. Needham, S. Pritchard, T. Li, R. Elmentaite, J. Park, E. Rahmani, D. Chen, D.K. Menon, O.A. Bayraktar, L. K. James, K.B. Meyer, N. Yosef, M.R. Clatworthy, P.A. Sims, D.L. Farber, K. Saeb-

Parsy, J.L. Jones, S.A. Teichmann, Cross-tissue immune cell analysis reveals tissue-specific features in humans, Science 376 (2022), eabl5197.
[31] J. Cao, M. Spielmann, X. Qiu, X. Huang, D.M. Ibrahim, A.J. Hill, F. Zhang, S. Mundlos, L. Christiansen, F.J. Steemers, C. Trapnell, J. Shendure, The single-cell transcriptional landscape of mammalian organogenesis, Nature 566 (2019) 496–502.
[32] Y. Hao, S. Hao, E. Andersen-Nissen, W.M. Mauck 3rd, S. Zheng, A. Butler, M.J. Lee, A.J. Wilk, C. Darby, M. Zager, P. Hoffman, M. Stoeckius, E. Papalexi, E.P. Mimitou, J. Jain, A. Srivastava, T. Stuart, L.M. Fleming, B. Yeung, A.J. Rogers, J. M. McElrath, C.A. Blish, R. Gottardo, P. Smibert, R. Satija, Integrated analysis of multimodal single-cell data, Cell 184 (2021) 3573–3587.e29.
[33] J.D. Storey, The positive false discovery rate: a Bayesian interpretation and the q-value, Ann. Stat. 31 (2003), 2013–2035.
[34] P.A.P. Moran, Notes on continuous stochastic phenomena, Biometrika 37 (1950) 17–23.
[35] P. Angerer, L. Haghverdi, M. Büttner, F.J. Theis, C. Marr, F. Buettner, destiny – diffusion maps for large-scale single-cell data in R, (2016)1241-3.
[36] R.A. Amezquita, V.J. Carey, L.N. Carpp, L. Geistlinger, A.T.L. Lun, F. Marini, K. Rue-Albrecht, D. Risso, C. Soneson, L. Waldron, H. Pagès, M. Smith, W. Huber, M. Morgan, R. Gottardo, S.C. Hicks, Orchestrating Single-Cell Analysis with Bioconductor 17 (2020) 137–145.
[37] C. Auffray, M.H. Sieweke, F. Geissmann, Blood monocytes: development, heterogeneity, and relationship with dendritic cells, Annu. Rev. Immunol. 27 (2009) 669–692.
[38] H.-K.M. Makinde, J.L.M. Dunn, G. Gadhvi, M. Carns, K. Aren, A.H. Chung, L. N. Muhammad, J. Song, C.M. Cuda, S. Dominguez, J.E. Pandolfino, J.E. Dematte D'Amico, G.S. Budinger, S. Assassi, T.M. Frech, D. Khanna, A. Shaeffer, H. Perlman, M. Hinchcliff, D.R. Winter, Three distinct transcriptional profiles of monocytes associate with disease activity in Scleroderma patients, Arthritis Rheumatol. 75 (2023) 595–608.
[39] K. Tretina, E.-S. Park, A. Maminska, J.D. MacMicking, Interferon-induced guanylate-binding proteins: guardians of host defense in health and disease, J. Exp. Med. 216 (2019) 482–500.
[40] M. Hill, S. Russo, D. Olivera, M. Malcuori, G. Galliussi, M. Segovia, The intracellular cation channel TMEM176B as a dual immunoregulator, Front. Cell Dev. Biol. 10 (2022), 1038429.
[41] A. Ivetic, H.L. Hoskins Green, S.J. Hart, L-selectin, A major regulator of leukocyte adhesion, migration and signaling, Front. Immunol. 10 (2019) 1068.
[42] M. Rudnik, F. Rolski, S. Jordan, T. Mertelj, M. Stellato, O. Distler, P. Blyszczuk, G. Kania, Regulation of monocyte adhesion and type I interferon signaling by CD52 in patients with systemic sclerosis, Arthritis Rheumatol. 73 (2021) 1720–1730.
[43] M. Frankenberger, T.P.J. Hofer, A. Marei, F. Dayyani, S. Schewe, C. Strasser, A. Aldraihim, F. Stanzel, R. Lang, R. Hoffmann, O. Prazeres da Costa, T. Buch, L. Ziegler-Heitbrock, Transcript profiling of CD16-positive monocytes reveals a unique molecular fingerprint, Eur. J. Immunol. 42 (2012) 957–974.
[44] A.S.J. Marshall, J.A. Willment, E. Pyz, K.M. Dennehy, D.M. Reid, P. Dri, S. Gordon, S.Y.C. Wong, G.D. Brown, Human MICL (CLEC12A) is differentially glycosylated and is down-regulated following cellular activation, Eur. J. Immunol. 36 (2006) 2159–2169.
[45] I. Rollinger-Holzinger, B. Eibl, M. Pauly, U. Griesser, F. Hentges, B. Auer, G. Pall, P. Schratzberger, D. Niederwieser, E.H. Weiss, H. Zwierzina, LST1: a gene with extensive alternative splicing and immunomodulatory Function1, J. Immunol. 164 (2000) 3169–3176.
[46] P. Provost, J. Doucet, A. Stock, G. Gerisch, B. Samuelsson, O. Rådmark, Coactosin-like protein, a human F-actin-binding protein: critical role of lysine-75, Biochem. J. 359 (2001) 255–263.
[47] J.J. Bravo-Cordero, M. Oser, X. Chen, R. Eddy, L. Hodgson, J. Condeelis, A novel spatiotemporal RhoC activation pathway locally regulates cofilin activity at invadopodia, Curr. Biol. 21 (2011) 635–644.
[48] M.R. McCann, R. Monemdjou, P. Ghassemi-Kakroodi, H. Fahmi, G. Perez, S. Liu, X. Shi-Wen, S.K. Parapuram, F. Kojima, C.P. Denton, D.J. Abraham, J. Martel-Pelletier, L.J. Crofford, A. Leask, M. Kapoor, mPGES-1 null mice are resistant to bleomycin-induced skin fibrosis, Arthritis Res. Ther. 13 (2011) R6.
[49] K. Yokoyama, H. Mitoma, S. Kawano, Y. Yamauchi, Q. Wang, M. Ayano, Y. Kimoto, N. Ono, Y. Arinobu, K. Akashi, T. Horiuchi, H. Niiro, CEACAM 1, 3, 5 and 6 -positive classical monocytes correlate with interstitial lung disease in early systemic sclerosis, Front. Immunol. 13 (2022), 1016914.
[50] A. Mantovani, S.K. Biswas, M.R. Galdiero, A. Sica, M. Locati, Macrophage plasticity and polarization in tissue repair and remodelling, J. Pathol. 229 (2013) 176–185.
[51] A. de Morrée, B. Flix, I. Bagaric, J. Wang, M. van den Boogaard, L. Grand Moursel, R.R. Frants, I. Illa, E. Gallardo, R. Toes, S.M. van der Maarel, Dysferlin regulates cell adhesion in human monocytes, J. Biol. Chem. 288 (2013) 14147–14157.
[52] M.C. Gingras, J.F. Margolin, Differential expression of multiple unexpected genes during U937 cell and macrophage differentiation detected by suppressive subtractive hybridization, Exp. Hematol. 28 (2000) 65–76.
[53] R.M. Nyamao, J. Wu, L. Yu, X. Xiao, F.-M. Zhang, Roles of DDX5 in the tumorigenesis, proliferation, differentiation, metastasis and pathway regulation of human malignancies, Biochim. Biophys. Acta, Rev. Cancer 1871 (2019) 85–98.
[54] J. Rachmilewitz, M.L. Tykocinski, Differential effects of chondroitin sulfates A and B on monocyte and B-cell activation: evidence for B-cell activation via a CD44-dependent pathway, Blood 92 (1998) 223–229.
[55] A. Bhattacharjee, M. Shukla, V.P. Yakubenko, A. Mulya, S. Kundu, M.K. Cathcart, IL-4 and IL-13 employ discrete signaling pathways for target gene expression in alternatively activated monocytes/macrophages, Free Radic. Biol. Med. 54 (2013) 1–16.
[56] F. Zhang, H. Wang, X. Wang, G. Jiang, H. Liu, G. Zhang, H. Wang, R. Fang, X. Bu, S. Cai, J. Du, TGF-β induces M2-like macrophage polarization via SNAIL-mediated suppression of a pro-inflammatory phenotype, Oncotarget 7 (2016) 52294–52306.
[57] Y. He, H. Hara, G. Núñez, Mechanism and regulation of NLRP3 inflammasome activation, Trends Biochem. Sci. 41 (2016) 1012–1021.
[58] D. González-Serna, C. Shi, M. Kerick, J. Hankinson, J. Ding, A. McGovern, M. Tutino, G. Villanueva Martin, N. Ortego-Centeno, J.L. Callejas, J. Martin, G. Orozco, Functional genomics in primary T cells and monocytes identifies mechanisms by which genetic susceptibility loci influence systemic sclerosis risk, Arthritis Rheumatol 75 (2023) 1007–1020.
[59] E. López-Isac, L. Bossini-Castillo, S.G. Guerra, C. Denton, C. Fonseca, S. Assassi, X. Zhou, M.D. Mayes, C.P. Simeón, N. Ortego-Centeno, I. Castellví, P. Carreira, Spanish Scleroderma Group, O. Gorlova, L. Beretta, A. Santaniello, C. Lunardi, R. Hesselstrand, A. Nordin, G. Riemekasten, T. Witte, N. Hunzelmann, A. Kreuter, J.H.W. Distler, A.E. Voskuyl, J. de Vries-Bouwstra, B.P. Koeleman, A. Herrick, J. Worthington, T.R.D.J. Radstake, J. Martin, Identification of IL12RB1 as a novel systemic sclerosis susceptibility locus, Arthritis Rheumatol. 66 (2014) 3521–3523.
[60] E. López-Isac, M. Acosta-Herrera, M. Kerick, S. Assassi, A.T. Satpathy, J. Granja, M. R. Mumbach, L. Beretta, C.P. Simeón, P. Carreira, N. Ortego-Centeno, I. Castellvi, L. Bossini-Castillo, F. David Carmona, G. Orozco, N. Hunzelmann, J.H.W. Distler, A. Franke, C. Lunardi, G. Moroncini, A. Gabrielli, J. de Vries-Bouwstra, C. Wijmenga, B.P.C. Koeleman, A. Nordin, L. Padyukov, A.-M. Hoffmann-Vold, B. Lie, S. Proudman, W. Stevens, M. Nikpour, T. Vyse, A.L. Herrick, J. Worthington, C.P. Denton, Y. Allanore, M.A. Brown, R.D. Timothy, C. Fonseca, H.Y. Chang, M.D. Mayes, J. Martin,GWAS for systemic sclerosis identifies multiple risk loci and highlights fibrotic and vasculopathy pathways, Nat. Commun. 10 (2019) 4955.
[61] T. Li, L. Ortiz-Fernández, E. Andrés-León, L. Ciudad, B.M. Javierre, E. López-Isac, A. Guillén-Del-Castillo, C.P. Simeón-Aznar, E. Ballestar, J. Martin, Epigenomics and transcriptomics of systemic sclerosis CD4+ T cells reveal long-range dysregulation of key inflammatory pathways mediated by disease-associated susceptibility loci, Genome Med. 12 (2020) 81.
[62] A. Lescoat, V. Lecureur, M. Roussel, B.L. Sunnaram, A. Ballerie, G. Coiffier, S. Jouneau, O. Fardel, T. Fest, P. Jégo, CD16-positive circulating monocytes and fibrotic manifestations of systemic sclerosis, Clin. Rheumatol. 36 (2017) 1649–1654.
[63] D. Nehar-Belaid, S. Hong, R. Marches, G. Chen, M. Bolisetty, J. Baisch, L. Walters, M. Punaro, R.J. Rossi, C.-H. Chung, R.P. Huynh, P. Singh, W.F. Flynn, J.-A. Tabanor-Gayle, N. Kuchipudi, A. Mejias, M.A. Collet, A.L. Lucido, K. Palucka, P. Robson, S. Lakshminarayanan, O. Ramilo, T. Wright, V. Pascual, J. F. Banchereau, Mapping systemic lupus erythematosus heterogeneity at the single-cell level, Nat. Immunol. 21 (2020) 1094–1106.
[64] W. Zheng, X. Wang, J. Liu, X. Yu, L. Li, H. Wang, J. Yu, X. Pei, C. Li, Z. Wang, M. Zhang, X. Zeng, F. Zhang, C. Wang, H. Chen, H.-Z. Chen, Single-cell analyses highlight the proinflammatory contribution of C1q-high monocytes to Behçet's disease, Proc. Natl. Acad. Sci. U. S. A. 119 (2022), e2204289119.
[65] T. Carvalheiro, S. Horta, J.A.G. van Roon, M. Santiago, M.J. Salvador, H. Trindade, T.R.D.J. Radstake, J.A.P. da Silva, A. Paiva, Increased frequencies of circulating CXCL10-, CXCL8- and CCL4-producing monocytes and Siglec-3-expressing myeloid dendritic cells in systemic sclerosis patients, Inflamm. Res. 67 (2018) 169–177.
[66] J.S. Berkowitz, T. Tabib, H. Xiao, G.M. Sadej, D. Khanna, P. Fuschiotti, R. A. Lafyatis, J. Das, Cell-type-specific biomarkers of systemic sclerosis disease severity capture cell-intrinsic and cell-extrinsic circuits, Arthritis Rheumatol. (2023).
[67] M. Wu, S. Assassi, Dysregulation of type 1 interferon signaling in systemic sclerosis: a promising therapeutic target? Curr Treatm Opt Rheumatol 7 (2021) 349–360.
[68] J. Yang, L. Zhang, C. Yu, X.-F. Yang, H. Wang, Monocyte and macrophage differentiation: circulation inflammatory monocyte as biomarker for inflammatory diseases, Biomark. Res. 2 (2014) 1.
[69] J.J. Belch, R. Madhok, B. Shaw, P. Leiberman, R.D. Sturrock, C.D. Forbes, Double-blind trial of CL115,347, a transdermally absorbed prostaglandin E2 analogue, in treatment of Raynaud's phenomenon, Lancet 1 (1985) 1180–1183.
[70] A. Koeberle, O. Werz, Perspective of microsomal prostaglandin E2 synthase-1 as drug target in inflammation-related disorders, Biochem. Pharmacol. 98 (2015) 1–15.
[71] A. Koeberle, O. Werz, Perspective of microsomal prostaglandin E2 synthase-1 as drug target in inflammation-related disorders, Biochem. Pharmacol. 98 (2015) 1–15.
[72] E. López-Isac, L. Bossini-Castillo, C.P. Simeon, M.V. Egurbide, J.J. Alegre-Sancho, J.L. Callejas, J.A. Roman-Ivorra, M. Freire, L. Beretta, A. Santaniello, P. Airó, C. Lunardi, N. Hunzelmann, G. Riemekasten, T. Witte, A. Kreuter, J.H.W. Distler, A. J. Schuerwegh, M.C. Vonk, A.E. Voskuyl, P.G. Shiels, J.M. van Laar, C. Fonseca, C. Denton, A. Herrick, J. Worthington, S. Assassi, B.P. Koeleman, M.D. Mayes, T.R. D.J. Radstake, J. Martin, A genome-wide association study follow-up suggests a possible role for PPARG in systemic sclerosis susceptibility, Arthritis Res. Ther. 16 (2014) 2–9.
[73] F. Maione, G.M. Casillo, F. Raucci, A.J. Iqbal, N. Mascolo, The functional link between microsomal prostaglandin E synthase-1 (mPGES-1) and peroxisome proliferator-activated receptor γ (PPARγ) in the onset of inflammation, Pharmacol. Res. 157 (2020), 104807.
[74] F. Raucci, A. Saviano, G.M. Casillo, M. Guerra-Rodriguez, A.A. Mansour, M. Piccolo, M.G. Ferraro, E. Panza, V. Vellecco, C. Irace, F. Caso, R. Scarpa, N. Mascolo, M. Alfaifi, A.J. Iqbal, F. Maione, IL-17-induced inflammation modulates the mPGES-1/PPAR-γ pathway in monocytes/macrophages, Br. J. Pharmacol. 179 (2022) 1857–1873.
[75] D. Nehar-Belaid, S. Hong, R. Marches, G. Chen, M. Bolisetty, J. Baisch, L. Walters, M. Punaro, R.J. Rossi, C.-H. Chung, R.P. Huynh, P. Singh, W.F. Flynn, J.-

A. Tabanor-Gayle, N. Kuchipudi, A. Mejias, M.A. Collet, A.L. Lucido, K. Palucka, P. Robson, S. Lakshminarayanan, O. Ramilo, T. Wright, V. Pascual, J. F. Banchereau, Mapping systemic lupus erythematosus heterogeneity at the single-cell level, Nat. Immunol. 21 (2020) 1094–1106.

[76] W. Zheng, X. Wang, J. Liu, X. Yu, L. Li, H. Wang, J. Yu, X. Pei, C. Li, Z. Wang, M. Zhang, X. Zeng, F. Zhang, C. Wang, H. Chen, H.-Z. Chen, Single-cell analyses highlight the proinflammatory contribution of C1q-high monocytes to Behçet's disease, Proc. Natl. Acad. Sci. U. S. A. 119 (2022), e2204289119.

[77] W. Zheng, X. Wang, J. Liu, X. Yu, L. Li, H. Wang, J. Yu, X. Pei, C. Li, Z. Wang, M. Zhang, X. Zeng, F. Zhang, C. Wang, H. Chen, H.-Z. Chen, Single-cell analyses highlight the proinflammatory contribution of C1q-high monocytes to Behçet's disease, Proc. Natl. Acad. Sci. U. S. A. 119 (2022), e2204289119.

[78] F.D. Carmona, R. Gutala, C.P. Simeón, P. Carreira, N. Ortego-Centeno, E. Vicente-Rabaneda, F.J. García-Hernández, P. García de la Peña, M. Fernández-Castro, L. Martínez-Estupiñán, M.V. Egurbide, B.P. Tsao, P. Gourh, S.K. Agarwal, S. Assassi, M.D. Mayes, F.C. Arnett, F.K. Tan, J. Martín, Spanish Scleroderma Group, Novel identification of the IRF7 region as an anticentromere autoantibody propensity locus in systemic sclerosis, Ann. Rheum. Dis. 71 (2012) 114–119.

[79] Y. Liu, R. Lu, W. Cui, Y. Pang, C. Liu, L. Cui, T. Qian, L. Quan, Y. Dai, Y. Jiao, Y. Pan, X. Ye, J. Shi, Z. Cheng, L. Fu, High IFITM3 expression predicts adverse prognosis in acute myeloid leukemia, Cancer Gene Ther. 27 (2020) 38–44.

[80] A.D. Hoffmann, S.E. Weinberg, S. Swaminathan, S. Chaudhuri, H.F. Mubarak, M.J. Schipma, C. Mao, X. Wang, L. El-Shennawy, N.K. Dashzeveg, J. Wei, P.J. Mehl, L.J. Shihadah, C.M. Wai, C. Ostiguin, Y. Jia, P. D'Amico, N.R. Wang, Y. Luo, A.R. Demonbreun, M.G. Ison, H. Liu, D. Fang, Unique Molecular Signatures Sustained in Circulating Monocytes and Regulatory T Cells in Convalescent COVID-19 Patients, Clin Immunol, 252(2022)109634.

[81] G. Shi, S. Ozog, B.E. Torbett, A.A. Compton, mTOR inhibitors lower an intrinsic barrier to virus infection mediated by IFITM3, Proc. Natl. Acad. Sci. U. S. A. 115 (2018), E10069–E10078.

[82] D. Benfaremo, S. Svegliati, C. Paolini, S. Agarbati, G. Moroncini, Systemic sclerosis: from pathophysiology to novel therapeutic approaches, Biomedicines 10 (2022) 163.

[83] V. Sundblad, R.A. Gomez, J.C. Stupirski, P.F. Hockl, M.S. Pino, H. Laborde, G. A. Rabinovich, Circulating galectin-1 and galectin-3 in sera from patients with systemic sclerosis: associations with clinical features and treatment, Front. Pharmacol. 12 (2021), 650605.

[84] M.N. Negedu, C.A. Duckworth, L.-G. Yu, Galectin-2 in health and diseases, Int. J. Mol. Sci. 24 (2022) 341.

[85] D. Paclik, L. Werner, O. Guckelberger, B. Wiedenmann, A. Sturm, Galectins distinctively regulate central monocyte and macrophage function, Cell. Immunol. 271 (2011) 97–103.

[86] M. Uhlén, L. Fagerberg, B.M. Hallström, C. Lindskog, P. Oksvold, A. Mardinoglu, Å. Sivertsson, C. Kampf, E. Sjöstedt, A. Asplund, I. Olsson, K. Edlund, E. Lundberg, S. Navani, C.A.-K. Szigyarto, J. Odeberg, D. Djureinovic, J.O. Takanen, S. Hober, T. Alm, P.-H. Edqvist, H. Berling, H. Tegel, J. Mulder, J. Rockberg, P. Nilsson, J. M. Schwenk, M. Hamsten, K. von Feilitzen, M. Forsberg, L. Persson, F. Johansson, M. Zwahlen, G. von Heijne, J. Nielsen, F. Pontén, Proteomics. Tissue-based map of the human proteome, Science 347 (2015), 1260419.

[87] P. Laurent, V. Sisirak, E. Lazaro, C. Richez, P. Duffau, P. Blanco, M.-E. Truchetet, C. Contin-Bordes, Innate immunity in systemic sclerosis fibrosis: recent advances, Front. Immunol. 9 (2018) 1702.

[88] C. Yıldırım, D.Y.S. Vogel, M.R. Hollander, J.M. Baggen, R.D. Fontijn, S. Nieuwenhuis, A. Haverkamp, M.R. de Vries, P.H.A. Quax, J.J. Garcia-Vallejo, A. M. van der Laan, C.D. Dijkstra, T.C.T.M. van der Pouw Kraan, N. van Royen, A.J. G. Horrevoets, Galectin-2 induces a proinflammatory, anti-arteriogenic phenotype in monocytes and macrophages, PLoS One 10 (2015), e0124347.

[89] J. Kane, M. Jansen, S. Hendrix, L.A. Bosmans, L. Beckers, C. van Tiel, M. Gijbels, N. Zelcer, C.J. de Vries, P. von Hundelshausen, M. Vervloet, E. Eringa, A. J. Horrevoets, N. van Royen, E. Lutgens, Anti-Galectin-2 antibody treatment reduces atherosclerotic plaque size and alters macrophage polarity, Thromb. Haemostasis 122 (2022) 1047–1057.

[90] N. Higashi-Kuwata, T. Makino, Y. Inoue, M. Takeya, H. Ihn, Alternatively activated macrophages (M2 macrophages) in the skin of patient with localized scleroderma, Exp. Dermatol. 18 (2009) 727–729.

[91] T. Rőszer, Understanding the mysterious M2 macrophage through activation markers and effector mechanisms, Mediat. Inflamm. 2015 (2015), 816460.

[92] A. van Caam, J. Aarts, T. van Ee, E. Vitters, M. Koenders, F. van de Loo, P. van Lent, F. van den Hoogen, R. Thurlings, M.C. Vonk, P.M. van der Kraan, TGFβ-mediated expression of TGFβ-activating integrins in SSc monocytes: disturbed activation of latent TGFβ? Arthritis Res. Ther. 22 (2020) 42.

[93] F. Zhang, H. Wang, X. Wang, G. Jiang, H. Liu, G. Zhang, H. Wang, R. Fang, X. Bu, S. Cai, J. Du, TGF-β induces M2-like macrophage polarization via SNAIL-mediated suppression of a pro-inflammatory phenotype, Oncotarget 7 (2016) 52294–52306.

[94] X. Yang, H. Liu, T. Ye, C. Duan, P. Lv, X. Wu, J. Liu, K. Jiang, H. Lu, H. Yang, D. Xia, E. Peng, Z. Chen, K. Tang, Z. Ye, AhR activation attenuates calcium oxalate nephrocalcinosis by diminishing M1 macrophage polarization and promoting M2 macrophage polarization, Theranostics 10 (2020) 12011–12025.

[95] S. Pennathur, K. Pasichnyk, N.M. Bahrami, L. Zeng, M. Febbraio, I. Yamaguchi, D. M. Okamura, The macrophage phagocytic receptor CD36 promotes fibrogenic pathways on removal of apoptotic cells during chronic kidney injury, Am. J. Pathol. 185 (2015) 2232–2245.

[96] P. Laurent, J. Lapoirie, D. Leleu, E. Levionnois, C. Grenier, B. Jurado-Mestre, E. Lazaro, P. Duffau, C. Richez, J. Seneschal, J.-L. Pellegrin, J. Constans, T. Schaeverbeke, I. Douchet, D. Duluc, T. Pradeu, C. Chizzolini, P. Blanco, M.-E. Truchetet, C. Contin-Bordes, Fédération Hospitalo-Universitaire ACRONIM and the Centre National de Référence des Maladies Auto-Immunes Systémiques Rares de l'Est et du Sud-Ouest (RESO), Interleukin-1β-Activated Microvascular Endothelial Cells Promote DC-SIGN-Positive Alternatively Activated Macrophages as a Mechanism of Skin Fibrosis in Systemic Sclerosis, Arthritis Rheumatol. 74 (2022) 1013–1026.

[97] A. Masuda, H. Yasuoka, T. Satoh, Y. Okazaki, Y. Yamaguchi, M. Kuwana, Versican is upregulated in circulating monocytes in patients with systemic sclerosis and amplifies a CCL2-mediated pathogenic loop, Arthritis Res. Ther. 15 (2013) R74.

[98] C. Maier, A. Ramming, C. Bergmann, R. Weinkam, N. Kittan, G. Schett, J.H. W. Distler, C. Beyer, Inhibition of phosphodiesterase 4 (PDE4) reduces dermal fibrosis by interfering with the release of interleukin-6 from M2 macrophages, Ann. Rheum. Dis. 76 (2017) 1133–1141.